Effective hole extraction using MoOx-Al contact in perovskite CH3NH3PbI3 solar cells

Yixin Zhao, Alexandre M. Nardes, and Kai Zhu

Citation: Applied Physics Letters **104**, 213906 (2014); doi: 10.1063/1.4880899
View online: http://dx.doi.org/10.1063/1.4880899
View Table of Contents: http://scitation.aip.org/content/aip/journal/apl/104/21?ver=pdfcov
Published by the AIP Publishing

Effective hole extraction using MoO_x-Al contact in perovskite $CH_3NH_3PbI_3$ solar cells

Yixin Zhao, Alexandre M. Nardes, and Kai Zhu[a)]
Chemical and Materials Science Center, National Renewable Energy Laboratory, Golden, Colorado 80401, USA

(Received 5 April 2014; accepted 19 May 2014; published online 30 May 2014)

We report an 11.4%-efficient perovskite $CH_3NH_3PbI_3$ solar cell using low-cost molybdenum oxide/aluminum (i.e., MoO_x/Al) as an alternative top contact to replace noble/precious metals (e.g., Au or Ag) for extracting photogenerated holes. The device performance of perovskite solar cells using a MoO_x/Al top contact is comparable to that of cells using the standard Ag top contact. Analysis of impedance spectroscopy measurements suggests that using 10-nm-thick MoO_x and Al does not affect charge-recombination properties of perovskite solar cells. Using a thicker (20-nm) MoO_x layer leads to a lower cell performance caused mainly by a reduced fill factor. Our results suggest that MoO_x/Al is promising as a low-cost and effective hole-extraction contact for perovskite solar cells. [http://dx.doi.org/10.1063/1.4880899]

In the early 1990s, the optoelectronic properties of organic-inorganic halide perovskites were extensively studied mainly for light-emitting diodes and field-effect transistors.[1,2] Until very recently, three-dimensional halide perovskites (e.g., $CH_3NH_3PbI_3$) have emerged as a promising class of light absorbers with an exceptional, unparalleled progress in photovoltaic (PV) cell performance from 3.8% in 2009 (Ref. 3) to a certified 16.2% in 2013.[4] An open-circuit voltage of 1.13 V has been demonstrated with a 1.55-eV bandgap perovskite absorber.[5] Halide perovskites consist of Earth-abundant elements and have the capability of bandgap tuning by tailoring their inorganic and organic components.[6,7] Moreover, high-efficiency perovskite solar cells can be made by low-cost solution processing or simple physical vapor deposition.[8,9] Halide perovskites are not only direct-bandgap absorbers with strong absorption coefficients[10] but also they demonstrate long electron and hole diffusion lengths.[11,12] During the past couple years, halide perovskites have attracted enormous worldwide attention focusing on both perovskite material/device development and a fundamental understanding of materials properties and device operation principles.[5,6,10,13–21]

At present, perovskite solar cells are often made with two types of common device architectures, i.e., either mesostructured or planar thin-film solar cells. The first type is similar to the conventional solid-state dye-sensitized solar cells (DSSCs). A key component of this device configuration is a mesoporous metal-oxide (e.g., TiO_2) layer that is first coated with nanostructured perovskite absorbers and then infiltrated with a hole transport material (HTM, e.g., spiro-MeOTAD).[22] In addition to being the light absorber, perovskite can also be used as a hole conductor. In this situation, the standard HTM layer can be avoided.[13,23] For the planar perovskite solar cells, a thin layer (a few hundred nanometers) of perovskite absorber is sandwiched between the electron- and hole-contact layers (e.g., TiO_2 and spiro-MeOTAD, respectively). For both mesostructured and planar perovskite solar cells, a layer (about 80–150 nm thick) of Au or Ag is often used as the top metal contact for carrier extraction. Replacing Au or Ag with a low-cost material/structure that can also effectively extract photogenerated holes would help reduce the overall cost for producing perovskite solar cells.

In this paper, we demonstrate that a thin layer (10 nm) of molybdenum oxide (MoO_x) coupled with Al can be used as an effective top-contact structure for extracting photogenerated holes from perovskite $CH_3NH_3PbI_3$ solar cells. In recent years, transition metal oxides (TMO, e.g., MoO_x) have been used as either an interlayer or buffer layer for a variety of optoelectronic devices to improve either hole injection (e.g., in organic light-emitting diodes[24]) or hole extraction (e.g., in organic photovoltaics,[25] CdTe,[26] Si,[27] and quantum-dot solar cells[28]). We find that the device performance of perovskite solar cells using a MoO_x/Al top contact is comparable to that of cells using the standard Ag top contact. Analysis of impedance spectroscopy (IS) measurements shows that using 10-nm-thick MoO_x and Al does not affect charge-recombination properties. However, a thicker (20-nm) MoO_x layer leads to decreased cell performance resulting primarily from a reduced fill factor (FF).

The precursor of CH_3NH_3I was synthesized and purified as previously reported.[29] The pre-patterned fluorine-doped SnO_2 (FTO) coated glass substrate (TEC15, Hartford, USA) was coated with a compact TiO_2 layer by spray pyrolysis using 0.2 M Ti(IV) bis(ethyl acetoacetate)-diisopropoxide in 1-butanol at 450 °C. A mixture of $PbCl_2$ and CH_3NH_3I (1:3 molar ratio) was dissolved in dimethylformamide (DMF) to form the precursor solution,[5,30] which was spin-coated onto the TiO_2/FTO substrate at 2500 rpm for 10 s, followed by annealing at 100 °C for 45 min in air. A spiro-MeOTAD-based HTM solution with a previously reported recipe was spin-coated on the perovskite-covered TiO_2 electrodes at 4000 rpm for 30 s.[31] A thin layer (0–20 nm) of MoO_x was deposited by thermal evaporation. Finally, a 150-nm-thick metal (Ag or Al) layer was deposited by thermal evaporation. The active area of each device was about 0.2–0.3 cm^2. The X-ray diffraction (XRD) patterns of the perovskite films were conducted using Rigaku D/Max 2200 diffractometer with Cu K_α radiation. The ultraviolet/visible (UV/vis)

a)Author to whom correspondence should be addressed. Electronic mail: Kai.Zhu@nrel.gov

spectra were characterized by an ultraviolet/visible-near infrared (UV/vis-NIR) spectrophotometer (Cary-6000i). The morphology of perovskite film was examined by a field-emission scanning electron microscopy (FE-SEM, JEOL JSM-7000F). The photocurrent density–voltage (J–V) characteristics of perovskite solar cells were studied using a class AAA solar simulator (Oriel Sol3A). IS was done with a PARSTAT 2273 workstation with the frequency range of 0.1 Hz–100 kHz and modulation amplitude of 10 mV.

Fig. 1 displays the XRD patterns of a perovskite $CH_3NH_3PbI_3$ film deposited on a compact TiO_2 layer on the FTO-coated glass substrate. We observe characteristic perovskite diffraction peaks (denoted by stars) at about 14.1°, 28.44°, 31.88°, and 43.24°, respectively, corresponding to the diffractions from (110), (220), (310), and (314) crystal planes of the $CH_3NH_3PbI_3$ perovskite structure. The positions of these diffraction peaks are consistent with the previous reports.[30,31] The other XRD peaks are attributable to the TiO_2/FTO substrate.[30] No secondary phases (e.g., PbI_2) are found. The typical UV-vis absorption spectrum for the same perovskite $CH_3NH_3PbI_3$ film is shown in the inset of Fig. 1. Consistent with our previous reports,[29,32] the $CH_3NH_3PbI_3$ film strongly absorbs the illumination below 600 nm. The absorbance of $CH_3NH_3PbI_3$ decreases slightly with increasing wavelength from about 600 to 750 nm and then drops rapidly when the wavelength approaches the bandgap near 800 nm.

Fig. 2(a) shows the typical cross-sectional SEM image of the planar perovskite $CH_3NH_3PbI_3$ solar cell with the following layered structure: FTO/compact TiO_2/perovskite absorber/spiro-MeOTAD/MoO_x/metal. In this study, the metal layer is either Ag or Al. Although it is not evident in the SEM image, a 10-nm MoO_x interlayer is deposited by thermal evaporation between the spiro-MeOTAD and metal layers. The average thickness of the $CH_3NH_3PbI_3$ layer is about 300 nm, and the average thickness of the HTM layer (spiro-MeOTAD) is about 280 nm. In Fig. 2(b), we test the effect of MoO_x interlayer thickness on the J–V characteristics of perovskite $CH_3NH_3PbI_3$ solar cells using the Ag top contact. In the absence of MoO_x, the device displays a short-circuit photocurrent density (J_{sc}) of 19.94 mA/cm^2, open-circuit voltage (V_{oc})

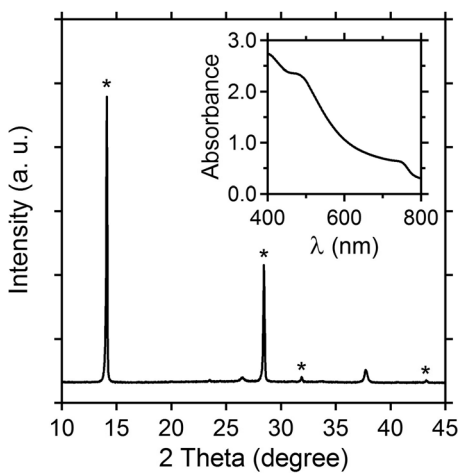

FIG. 1. XRD patterns and UV-vis absorption spectra of perovskite $CH_3NH_3PbI_3$ deposited on a compact TiO_2 layer on the FTO substrate. XRD peaks associated with the perovskite structure are labeled with stars. The other peaks are associated with the TiO_2/FTO substrate.

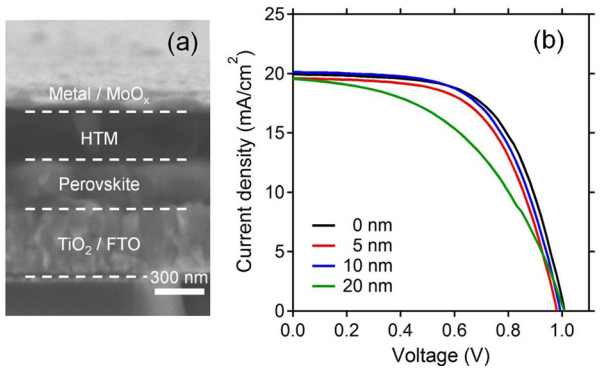

FIG. 2. (a) Typical cross-sectional SEM image of a planar FTO/TiO_2/$CH_3NH_3PbI_3$/spiro-MeOTAD/MoO_x/Metal (Ag or Al) solar cell. (b) Effect of MoO_x interlayer thickness on the J–V characteristics of perovskite $CH_3NH_3PbI_3$ solar cells using Ag top contact.

of 1.011 V, and FF of 0.613 to yield an efficiency (η) of 12.36%. When 5-nm and 10-nm MoO_x layers are used, the respective efficiencies are 11.49% and 12.04%. The mean values and standard deviations of the PV parameters from 8 to 20 cells for these device architectures are given in Table I. It is evident that the 5-nm and 10-nm MoO_x cells have essentially the same performance level as the cell without the MoO_x layer, within experimental error. However, when a 20-nm-thick MoO_x layer is used, the cell efficiency is significantly reduced from about 12% to 9.33%. The decrease of cell efficiency is primarily caused by the much reduced FF, which is in agreement with a recent study on the effect of MoO_x layer thickness on the device characteristics of Si solar cells.[27] The details of the photovoltaic parameters (J_{sc}, V_{oc}, FF, and η) for all these cells are given in Table I.

Having established that MoO_x works as an effective interlayer for hole extraction in our regular device architecture, we compare in Fig. 3(a) the J–V characteristics of perovskite $CH_3NH_3PbI_3$ solar cells using different top-contact structures, including: (1) HTM/Ag, (2) HTM/MoO_x/Ag, (3) HTM/MoO_x/Al, (4) HTM/Al, and (5) MoO_x/Ag (no HTM). For top-contact structures (2), (3), and (5), we used a fixed 10-nm-thick MoO_x layer. The composition of the spiro-MeOTAD-based HTM layer is given in detail in the experimental section. Using the HTM/MoO_x/Al contact structure, the cell efficiency is 11.42% with a J_{sc} of 19.55 mA/cm^2, V_{oc} of 0.990 V, and FF of 0.590. All of these parameters are comparable to those of the cells using HTM/Ag and HTM/MoO_x/Ag contact structures (Table I). Consistent with the J–V results, the incident photon-to-current efficiency (IPCE) spectra for cells based on contact structures (1)–(3) are essentially identical (Fig. 3(b)). These results suggest that the junction between MoO_x and the metal contact is not critical to hole extraction in perovskite solar cells. This observation agrees with other studies where MoO_x is used as an interlayer in organic solar cells[33] and quantum-dot solar cells[28] to facilitate extraction of photogenerated holes. It is worth noting that these studies demonstrated improved cell performance using the MoO_x interlayer than the control sample without the MoO_x layer. In contrast, our study shows that cells using HTM/MoO_x/Ag or HTM/MoO_x/Al have comparable performance to the control cells using HTM/Ag. This is presumably caused by the use of HTM in this study,

TABLE I. Effect of the top layer (hole-contact) structure on the short-circuit photocurrent density J_{sc}, open-circuit voltage V_{oc}, fill factor FF, and conversion efficiency η of champion planar perovskite $CH_3NH_3PbI_3$ solar cells. The mean values and standard deviations of the PV parameters from 8 to 20 cells for each type of devices are given in parentheses.

Cell type	J_{sc} (mA/cm^2)	V_{oc} (V)	FF	η (%)
HTM/Ag	19.94 (19.45 ± 0.90)	1.011 (0.967 ± 0.040)	0.613 (0.538 ± 0.043)	12.36 (10.13 ± 0.99)
HTM/5-nm MoO_x/Ag	19.60 (19.43 ± 0.60)	0.985 (0.952 ± 0.026)	0.595 (0.544 ± 0.027)	11.49 (10.08 ± 0.81)
HTM/10-nm MoO_x/Ag	20.14 (20.37 ± 0.95)	0.993 (0.962 ± 0.021)	0.602 (0.543 ± 0.036)	12.04 (10.63 ± 0.70)
HTM/20-nm MoO_x/Ag	19.56 (19.22 ± 0.82)	1.008 (0.964 ± 0.024)	0.473 (0.439 ± 0.025)	9.33 (8.15 ± 0.64)
HTM/10-nm MoO_x/Al	19.55 (19.31 ± 0.85)	0.990 (0.972 ± 0.023)	0.590 (0.542 ± 0.030)	11.42 (9.85 ± 0.91)
HTM/Al	0.92 (0.67 ± 0.26)	0.182 (0.119 ± 0.104)	0.165 (0.203 ± 0.060)	0.027 (0.015 ± 0.011)
10-nm MoO_x/Ag	0.84 (0.66 ± 0.13)	0.045 (0.034 ± 0.016)	0.261 (0.254 ± 0.025)	0.01 (0.006 ± 0.003)

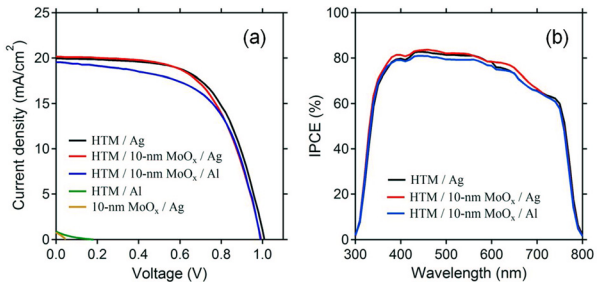

FIG. 3. Comparison of (a) J–V characteristics and (b) IPCE of perovskite $CH_3NH_3PbI_3$ solar cells using different top-contact structures as indicated.

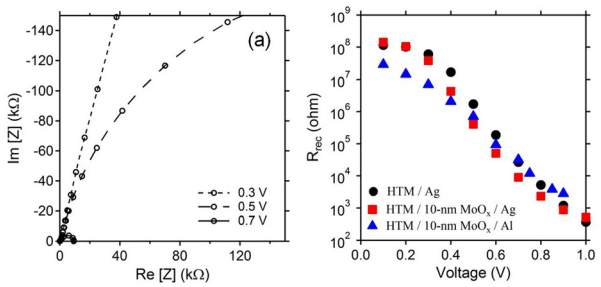

FIG. 4. (a) Typical Nyquist plots of the impedance responses (Z) for a planar perovskite cell (using HTM/10-nm MoO_x/Ag) with three different bias voltages. (b) Comparison of recombination resistance (R_{rec}) as a function of voltage for planar perovskite solar cells using different top-contact structures as indicated.

whereas in other studies the MoO_x layer is deposited directly on the absorber layer. Interestingly, we find that when Al is deposited directly on top of the HTM layer (i.e., no MoO_x is used), the perovskite solar cell only shows a conversion efficiency of 0.027% with a J_{sc} of 0.92 mA/cm^2, V_{oc} of 0.182 V, and FF of 0.165. This could be attributed to the formation of a back diode at the HTM/Al interface, which creates an energy barrier limiting hole extraction.[28] It was shown previously for PbS quantum dot solar cells that the back-diode effect can be significantly reduced when using higher work-function metals (e.g., Au or Ag) or can be completely removed by using a MoO_x interlayer.[28] It is worth noting that using MoO_x/Ag directly on the perovskite absorber layer (i.e., no HTM layer) leads to a 0.01% device (Table I). This is presumably caused by shorting associated with pinholes on the absorber layer. The use of the HTM layer appears to be effective in suppressing shorting in perovskite cells.

Impedance spectroscopy[17,22,34] is used to study the impact of top-contact structure on the recombination resistance (R_{rec}) for the perovskite solar cells. Fig. 4(a) shows the typical Nyquist plots of the complex impedance Z (i.e., the imaginary component Im [Z] versus the real component Re [Z] of the impedance) for a perovskite cell with three different bias voltages. The impedance spectra are dominated by a large semicircle at low frequencies. This feature has been attributed to charge recombination either at the interface between perovskite and contact layers or within the bulk perovskite layer.[34] A larger semicircle corresponds to a larger recombination resistance R_{rec}, which is inversely proportional to the recombination rate. The model used for impedance analysis has been previously discussed in detail by others.[17,34,35] From these Nyquist plots, the recombination resistance of the perovskite cells can be determined. Fig. 4(b) shows the R_{rec} values as a function of voltage for perovskite solar cells using the top-contact structures (1)–(3). The R_{rec} for all these cell structures depends strongly on the bias voltage, following an approximately exponential decrease with voltage. Similar voltage dependence of recombination resistance for perovskite solar cells has been reported previously.[22] Interestingly, there is not much difference in recombination resistance among the three samples despite the significant difference in their top-contact structures, which suggests that the MoO_x/metal interface does not affect charge transfer at the back contact. This is in agreement with the J–V measurements in Fig. 3(a). Thus, the J–V and impedance results suggest that MoO_x/Al can be used as an effective hole-extraction contact to replace more expensive metal contacts (e.g., Ag or Au) for perovskite solar cells.

In summary, we demonstrate the effectiveness of using a combination of a thin layer of molybdenum oxide and aluminum as the top-contact structure for extracting photogenerated holes from perovskite solar cells. MoO_x is deposited by thermal evaporation. The device performance of perovskite solar cells using a MoO_x/Al top contact is comparable to that of cells using the standard Ag top contact. Impedance measurements suggest that the extraction of photogenerated holes is not affected by the MoO_x/metal interface when proper MoO_x thickness (e.g., 10 nm) is used. Using a thicker (20-nm) MoO_x layer leads to decreased cell performance resulting primarily from a reduced fill factor.

We acknowledge the support by the U.S. Department of Energy/National Renewable Energy Laboratory's Laboratory Directed Research and Development (LDRD) program under Contract No. DE-AC36-08GO28308.

[1]D. B. Mitzi, C. A. Feild, W. T. A. Harrison, and A. M. Guloy, Nature **369**, 467 (1994).
[2]T. Ishihara, J. Lumin. **60–61**, 269 (1994).
[3]A. Kojima, K. Teshima, Y. Shirai, and T. Miyasaka, J. Am. Chem. Soc. **131**, 6050 (2009).
[4]H.-S. Kim, S. H. Im, and N.-G. Park, J. Phys. Chem. C **118**, 5615 (2014).
[5]M. M. Lee, J. Teuscher, T. Miyasaka, T. N. Murakami, and H. J. Snaith, Science **338**, 643 (2012).
[6]J. H. Noh, S. H. Im, J. H. Heo, T. N. Mandal, and S. I. Seok, Nano Lett. **13**, 1764 (2013).
[7]G. E. Eperon, S. D. Stranks, C. Menelaou, M. B. Johnston, L. M. Herz, and H. J. Snaith, Energy Environ. Sci. **7**, 982 (2014).
[8]J. Burschka, N. Pellet, S. J. Moon, R. Humphry-Baker, P. Gao, M. K. Nazeeruddin, and M. Gratzel, Nature **499**, 316 (2013).
[9]M. Liu, M. B. Johnston, and H. J. Snaith, Nature **501**, 395 (2013).
[10]J.-H. Im, C.-R. Lee, J.-W. Lee, S.-W. Park, and N.-G. Park, Nanoscale **3**, 4088 (2011).
[11]G. Xing, N. Mathews, S. Sun, S. S. Lim, Y. M. Lam, M. Gratzel, S. Mhaisalkar, and T. C. Sum, Science **342**, 344 (2013).
[12]S. D. Stranks, G. E. Eperon, G. Grancini, C. Menelaou, M. J. P. Alcocer, T. Leijtens, L. M. Herz, A. Petrozza, and H. J. Snaith, Science **342**, 341 (2013).
[13]W. Abu Laban and L. Etgar, Energy Environ. Sci. **6**, 3249 (2013).
[14]B. Cai, Y. Xing, Z. Yang, W.-H. Zhang, and J. Qiu, Energy Environ. Sci. **6**, 1480 (2013).
[15]J. Qiu, Y. Qiu, K. Yan, M. Zhong, C. Mu, H. Yan, and S. Yang, Nanoscale **5**, 3245 (2013).
[16]D. Bi, L. Yang, G. Boschloo, A. Hagfeldt, and E. M. J. Johansson, J. Phys. Chem. Lett. **4**, 1532 (2013).
[17]J. A. Christians, R. C. M. Fung, and P. V. Kamat, J. Am. Chem. Soc. **136**, 758 (2014).
[18]Q. Chen, H. Zhou, Z. Hong, S. Luo, H.-S. Duan, H.-H. Wang, Y. Liu, G. Li, and Y. Yang, J. Am. Chem. Soc. **136**, 622 (2014).
[19]E. Edri, S. Kirmayer, D. Cahen, and G. Hodes, J. Phys. Chem. Lett. **4**, 897 (2013).
[20]W. J. Yin, T. T. Shi, and Y. F. Yan, Appl. Phys. Lett. **104**, 063903 (2014).
[21]S. Colella, E. Mosconi, P. Fedeli, A. Listorti, F. Gazza, F. Orlandi, P. Ferro, T. Besagni, A. Rizzo, G. Calestani, G. Gigli, F. De Angelis, and R. Mosca, Chem. Mater. **25**, 4613 (2013).
[22]H.-S. Kim, C.-R. Lee, J.-H. Im, K.-B. Lee, T. Moehl, A. Marchioro, S.-J. Moon, R. Humphry-Baker, J.-H. Yum, J. E. Moser, M. Gratzel, and N.-G. Park, Sci. Rep. **2**, 591 (2012).
[23]J. Shi, J. Dong, S. Lv, Y. Xu, L. Zhu, J. Xiao, X. Xu, H. Wu, D. Li, Y. Luo, and Q. Meng, Appl. Phys. Lett. **104**, 063901 (2014).
[24]M. Vasilopoulou, G. Papadimitropoulos, L. C. Palilis, D. G. Georgiadou, P. Argitis, S. Kennou, I. Kostis, N. Vourdas, N. A. Stathopoulos, and D. Davazoglou, Org. Electron. **13**, 796 (2012).
[25]B. Dasgupta, W. P. Goh, Z. E. Ooi, L. M. Wong, C. Y. Jiang, Y. Ren, E. S. Tok, J. Pan, J. Zhang, and S. Y. Chiam, J. Phys. Chem. C **117**, 9206 (2013).
[26]C. Gretener, J. Perrenoud, L. Kranz, C. Baechler, S. Yoon, Y. E. Romanyuk, S. Buecheler, and A. N. Tiwari, Thin Solid Films **535**, 193 (2013).
[27]C. Battaglia, S. M. de Nicolás, S. De Wolf, X. Yin, M. Zheng, C. Ballif, and A. Javey, Appl. Phys. Lett. **104**, 113902 (2014).
[28]J. Gao, C. L. Perkins, J. M. Luther, M. C. Hanna, H.-Y. Chen, O. E. Semonin, A. J. Nozik, R. J. Ellingson, and M. C. Beard, Nano Lett. **11**, 3263 (2011).
[29]Y. Zhao and K. Zhu, J. Phys. Chem. Lett. **4**, 2880 (2013).
[30]A. Dualeh, N. Tétreault, T. Moehl, P. Gao, M. K. Nazeeruddin, and M. Grätzel, "Effect of annealing temperature on film morphology of organic–inorganic hybrid perovskite solid-state solar cells," Adv. Funct. Mater. (published online).
[31]Y. Zhao, A. M. Nardes, and K. Zhu, J. Phys. Chem. Lett. **5**, 490 (2014).
[32]Y. Zhao and K. Zhu, Chem. Commun. **50**, 1605 (2014).
[33]C. Tao, S. Ruan, X. Zhang, G. Xie, L. Shen, X. Kong, W. Dong, C. Liu, and W. Chen, Appl. Phys. Lett. **93**, 193307 (2008).
[34]E. J. Juarez-Perez, M. Wußler, F. Fabregat-Santiago, K. Lakus-Wollny, E. Mankel, T. Mayer, W. Jaegermann, and I. Mora-Sero, J Phys. Chem. Lett. **5**, 680 (2014).
[35]Y. Zhao and K. Zhu, J. Phys. Chem. C **118**, 9412 (2014).